A New Convexity Measurement for 3D Meshes

Zhouhui Lian[1], Afzal Godil[2], Paul L. Rosin[3], Xianfang Sun[3]
[1]Institute of Computer Science and Technology, Peking University, Beijing, China
[2]National Institute of Standards and Technology, Gaithersburg, USA
[3]Cardiff University, Wales, UK

Abstract

This paper presents a novel convexity measurement for 3D meshes. The new convexity measure is calculated by minimizing the ratio of the summed area of valid regions in a mesh's six views, which are projected on faces of the bounding box whose edges are parallel to the coordinate axes, to the sum of three orthogonal projected areas of the mesh. The complete definition, theoretical analysis, and a computing algorithm of our convexity measure are explicitly described. This paper also proposes a new 3D shape descriptor CD (i.e., Convexity Distribution) based on the distribution of above-mentioned ratios, which are computed by randomly rotating the mesh around its center, to better describe the object's convexity-related properties compared to existing convexity measurements. Our experiments not only show that the proposed convexity measure corresponds well with human intuition, but also demonstrate the effectiveness of the new convexity measure and the new shape descriptor by significantly improving the performance of other methods in the application of 3D shape retrieval.

1. Introduction

Shape measurement is a fundamental problem in several research communities including computer vision, pattern recognition, and computer graphics. It is often preferable if shapes can be quantified by some global shape measures with direct intuitive meanings, such as, chirality [17], compactness [32], convexity [34], ellipticity [18], rectangularity [21], rectilinearity [33], symmetry [9], triangularity [22], and so on. While a large amount of 2D shape measures have been proposed in the last few years, there has been much less work on the measurement of 3D shapes. This paper investigates the convexity for 3D polygon meshes.

Convexity is a basic and popular shape descriptor with many applications. As defined in [34] [19], an object is said to be convex if it contains all points on the line segment between any two points that belong to the object. The concept of convexity of 3D shapes is demonstrated by some simple

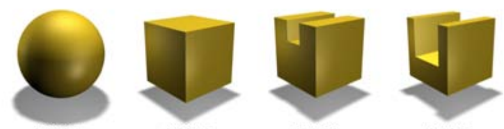

Figure 1. Sphere, cube and two concave 3D models. Underneath are their convexity values calculated using our method.

examples shown in Figure 1. Intuitively, the sphere and the cube are considered to be convex, while the other two are concave and the rightmost one should have a smaller value of convexity than its nearest neighbor. We would like to define a shape measure describing the extent to which a 3D object is convex. Trivially, the following two definitions can be obtained by directly generalizing 2D convexity measures [34] [19] into 3D domain.

Definition 1. For a given 3D closed mesh M, where the region bounded by the surface M is M_+, we define its convexity measure $C_1(M)$ as

$$C_1(M) = P(\alpha X_1 + (1-\alpha)X_2 \in M_+), \forall \alpha \in [0,1], \quad (1)$$

where $P(E)$ denotes the probability of event E, $\{\alpha X_1 + (1-\alpha)X_2; 0 \leq \alpha \leq 1\}$ is the line segment between any two points X_1 and X_2 randomly chosen on the surface M.

Definition 2. For a given 3D closed mesh M, where the convex hull of M is $CH(M)$, we define its convexity measure $C_2(M)$ as

$$C_2(M) = \frac{Volume(M)}{Volume(CH(M))}. \quad (2)$$

Although the above two definitions both satisfy necessary requirements (see [34]) for the convexity measurement, they also have their own limitations. In general, the computational cost of the statistics-based measure $C_1(M)$ is quite expensive. While the volume-based measure $C_2(M)$ is easy to calculate but it cannot always detect small defects of volume, even if the defects have a huge impact on the surface area of 3D models. That is indicated by two examples

978-1-4673-1228-8/12/$31.00 ©2012 IEEE

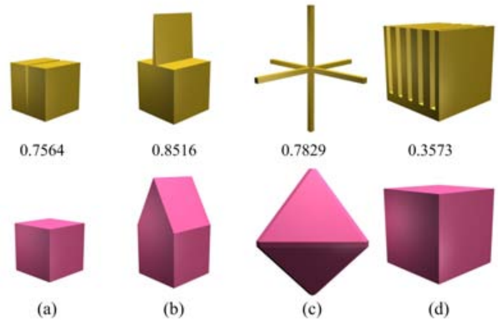

Figure 2. Examples of some particular models (first row) and their convex hulls (second row).Underneath of the original models are their convexity values obtained using our method.

shown in Figure 2(a)(b). As we can see, these two models (first row) have similar values of surface area and volume but quite different convex hulls (second row). When the volume of the deep indentation in Figure 2(a) tends to 0, the object's convexity calculated by $C_2(M)$ is arbitrary close to 1 although its depth remains unchanged. In other words, the measurement $C_2(M)$ is not able to detect deep but small-volume indentations into shapes. However, in some applications, we would like to have a 3D convexity measurement that is sensitive to all kinds of defects of surface. To the best of our knowledge, up to now, no boundary-based (i.e., area-based) convexity measure has been proposed for 3D shapes, and the boundary-based 2D convexity measure cannot be directly generalized into 3D. Recall that, for a given 2D polygon, its boundary-based convexity measure is defined as the ratio of the Euclidean perimeter of the boundary of its convex hull to that of the original 2D shape [34]. However, the surface area of a 3D mesh can be either smaller or larger than the surface area of its convex hull (see Figure 2(c)(d)), thereby neither $\frac{Area(M)}{Area(CH(M))}$ nor $\frac{Area(CH(M))}{Area(M)}$ is suitable to measure convexity for 3D shapes.

Furthermore, existing methods all calculate a single value to measure the convexity property of a given shape, and thus there exist lots of shapes that are quite different but still have the same convexity value obtained using those traditional methods. To address the problems mentioned above, this paper propose an area-based convexity measure and a new convexity-related shape descriptor for 3D meshes. Given a 3D model, the new convexity measure (see Figures 1and 2 for some computed results) is calculated by minimizing the ratio of the summed area of valid regions in six orthogonal views to the sum of three orthogonal projected areas, and the new shape descriptor CD (i.e., Convexity Distribution) is constructed based on the distribution of above-mentioned ratios computed by randomly rotating the mesh around its center. Since our convexity measure and shape descriptor both represent 3D models in quite different manners compared to other existing shape descriptors, and thus provide new and independent information, they are well suited to be incorporated with other shape descriptors to generate discriminative composite signatures. Our experiments validate the effectiveness of the proposed convexity measure and convexity distribution in the application of 3D shape retrieval.

2. Related Work

Convexity is one of the best-known global shape descriptors that have direct intuitive meanings. Up to now, a number of definitions of the convexity measure have been reported for 2D shapes. Among them, the mostly used method that appears in textbooks [26] defines the convexity of a 2D polygon as the ratio of the shape's area to the area of its convex hull. Similarly, the ratio between the Euclidean perimeter of a polygon's convex hull and the Euclidean perimeter of the polygon is also a natural solution to measure the convexity of 2D shapes [34]. Alternatively, according to the definition of convex shapes [34] [19], a convexity measure can directly be defined as the probability that, for randomly chosen points A and B in a 2D shape, all points on the line segment $[AB]$ belong to the shape [34]. There are also other 2D convexity measures whose definitions are not so intuitive. For example, Stern [27] developed an area-based convexity measure to incorporate the entire topology of the polygon. Boxer [1] estimated the convexity of a given 2D polygon based on the distances between the vertices of the polygon and its convex hull. Recently, Žunić and Rosin [34] presented a boundary-based method to measure convexity by using the minimum ratio of the Euclidean perimeter of the bounding rectangle of a polygon to the polygon's L_1 perimeter. Rahtu *et al.* [19] proposed a convexity measure based on the idea of randomly choosing pairs of points from a 2D object and then computing the probability that a point located on the specified position of corresponding line segments belongs to the shape. One merit of this method is that it can be implemented efficiently using the Fast Fourier Transform. Rosin and Mumford [23] introduced a symmetric convexity measure that is based on the maximally overlapping convex polygon of a 2D shape.

However, there has been considerably less work for the shape measurement of 3D shapes. Regarding convexity, besides the two intuitive definitions presented in Section 1, Rahtu *et al.* [19] generalized their probability-based method to measure the convexity of N-dimensional data, while Fink and Wood [5] developed a restricted-orientation convexity which was defined in terms of the intersection of a geometric object with lines parallel to the elements of a fixed orientation set. In recent years, more and more researchers have become interested in 3D shape measurements. For instance, Bribiesca [2] proposed a compactness measure which corresponds to the sum of the contact surface areas of the face-connected voxels for 3D shapes. Kazhdan *et al.* [8] presented a 3D object's reflective symmetry descriptor as a 2D function associating a measurement of reflective symmetry to every plane through the model's centroid. Lian *et al.* [12] proposed a rectilinearity measure for 3D polygon meshes, which is defined as the maximum ratio of the surface area to the sum of three orthogonal projected areas of the mesh. Motivated by the work presented in [34] and [12], this paper develops a new convexity measure for 3D meshes.

One potential application of shape measurements is 3D shape retrieval. Until recently, a large number of methods have been developed for the retrieval of 3D shapes, such as, D2 [16], SHD [8], LFD [3], and so on. Probably because of the complexity of non-rigid 3D shape analysis, previous efforts have mainly been devoted to rigid 3D shape retrieval (see [30] for more details). Thereby, how to effectively and efficiently calculate the dissimilarity between non-rigid models is still considered to be a challenging problem in content-based 3D object retrieval. Here, we briefly review some representative work published recently for the retrieval of non-rigid 3D shapes. Wang *et al.* [31] proposed to compare non-rigid 3D models based on a local feature named Intrinsic Spin Images (ISIs), which is designed by generalizing the traditional spin images [7] from 3D space to N-dimensional intrinsic shape space. Tam and Lau [29] used topological and geometric features simultaneously to search deformable 3D models. Mahmoudi and Sapiro [13] designed six isometric-invariant signatures by using the distributions of intrinsic distances. Mémoli and Sapiro [14] presented a theoretical framework to directly compare non-rigid 3D shapes based on the Gromov-Hausdorff (GH) distance. The above-mentioned algorithms are not well suited for practical use mainly due to the fact that they are either computationally expensive or poor in discrimination. Perhaps, the utilization of *Canonical Forms* is potentially the best way to address the problem of non-rigid shape matching. With the help of canonical forms, we can apply any shape searching method in the retrieval of non-rigid models. The idea of generating canonical forms in the 3D domain was initially proposed in [4], where the authors presented an invariant representation for isometric surfaces using Multidimensional Scaling (MDS) embedding of the surface in a low dimensional Euclidean space in which geodesic distances can be approximated by Euclidean ones. Excellent performance of non-rigid 3D shape retrieval was reported in [11], where Lian *et al.* described a visual similarity based framework by using the MDS canonical form and the Bag-of-features approach.

3. A New Convexity Measure for 3D Meshes

In this section, we first give some notations used in this paper and then present the definition of our new convexity measure with complete proofs. Throughout this paper, we assume that all considered shapes are 3D closed triangle meshes, which for convenience are directly called 3D meshes unless otherwise specified.

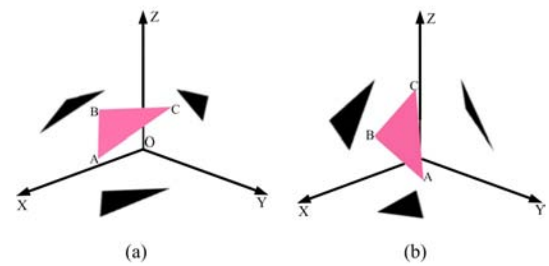

Figure 3. Projecting a triangle on three orthogonal planes. Rotation of the coordinate frame (b) results in different projected shapes compared to the original one (a).

Given a 3D mesh M, its three projected areas on the YOZ, ZOX, and XOY planes are denoted as $Pface_x(M)$, $Pface_y(M)$, and $Pface_z(M)$, respectively, while areas of valid regions in the views projected on those three orthogonal planes are $Pview_x(M)$, $Pview_y(M)$, and $Pview_z(M)$, respectively. More specifically, the projected area on a plane is equal to the sum of area of the projected region of every triangle face on the surface, and the area of the valid region in a view stands for the area of the polygon formed by projecting the whole mesh on a plane. Figure 3 displays the projections of single triangle faces, while Figure 4 shows some examples of silhouette views for whole objects.

If we rotate the coordinate frame, we will get new projected areas (see Figure 3) and new silhouette views (see Figure 4(b)(c)) of the mesh M. Therefore, we should use $Pface_x(M,\alpha,\beta,\gamma)$, $Pface_y(M,\alpha,\beta,\gamma)$, $Pface_z(M,\alpha,\beta,\gamma)$ for these three projected areas and $Pview_x(M,\alpha,\beta,\gamma)$, $Pview_y(M,\alpha,\beta,\gamma)$, $Pview_z(M,\alpha,\beta,\gamma)$ for areas of the valid regions in three views, after successively rotating the coordinate frame around its x,y, and z axes by angles α,β, and γ, respectively. We denote the sum of three projected areas as

$$Pface(M,\alpha,\beta,\gamma) = Pface_x(M,\alpha,\beta,\gamma) + Pface_y(M,\alpha,\beta,\gamma) + Pface_z(M,\alpha,\beta,\gamma), \quad (3)$$

while the sum of areas of the valid regions in six views projected on faces of the bounding box whose edges are parallel to the coordinate axes is defined as

$$Pview(M,\alpha,\beta,\gamma) = 2\cdot(Pview_x(M,\alpha,\beta,\gamma) + Pview_y(M,\alpha,\beta,\gamma) + Pview_z(M,\alpha,\beta,\gamma)). \quad (4)$$

Theorem 1. 1) The inequality

$$Pface(M,\alpha,\beta,\gamma) \geq Pview(M,\alpha,\beta,\gamma) \quad (5)$$

holds for any 3D closed mesh M.

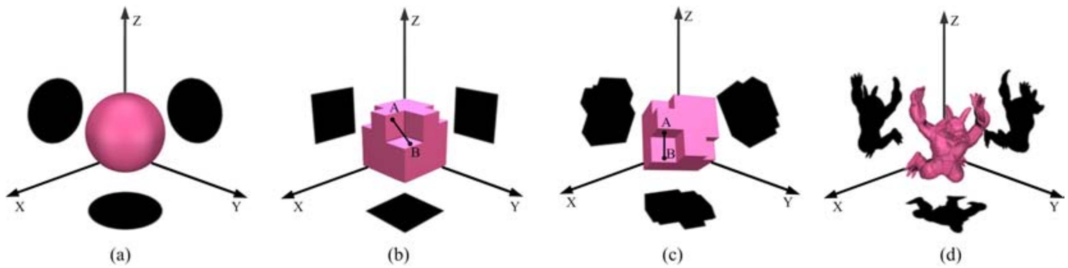

Figure 4. Projecting 3D models on three orthogonal planes. Models shown in (b) and (c) are the same, while the coordinate frame in (c) has been rotated to make its z axis be parallel to line segment $[AB]$.

2) A given 3D mesh M is convex if and only if for any choice of the coordinate frame the sum of three projected areas of M equals the sum of areas of the valid regions in six views projected on faces of the bounding box whose edges are parallel to the coordinate axes, i.e.,

$$\begin{aligned} Pface(M,\alpha,\beta,\gamma) &= Pview(M,\alpha,\beta,\gamma), \\ &\quad \forall\alpha,\beta,\gamma \in [0,2\pi]. \end{aligned} \tag{6}$$

Proof. On the one hand, if a given 3D mesh M is convex, then the projections of the faces of M onto the YOZ, ZOX, and XOY planes exactly cover the valid regions of six views projected on faces of the bounding box whose edges are parallel to the coordinate axes (see Figure 4(a)). Furthermore, such projections are independent of the choice of the coordinate system, i.e., $Pface(M,\alpha,\beta,\gamma) = Pview(M,\alpha,\beta,\gamma)$, for all $\alpha,\beta,\gamma \in [0,2\pi]$, when M is convex.

On the other hand, if M is not convex, then there exist points A and B on the mesh M such that the line segment $[AB]$ does not completely belong to M and its interior (see Figure 4(b)). Let a coordinate axis, say z, be parallel to the line through points A and B, then the projections of the faces of M onto the plane XOY must overlap (see Figure 4(c)). That is, $Pface(M,\alpha,\beta,\gamma) > Pview(M,\alpha,\beta,\gamma)$ for some or all α,β,γ. Moreover, the fact that M is a closed mesh means any point on the valid region of projected views has at least two corresponding points on the surface of M. In other words, $Pface(M,\alpha,\beta,\gamma)$ could never be smaller than $Pview(M,\alpha,\beta,\gamma)$. This complete the proof for both statement 1) and 2). □

Theorem 1 suggests that the ratio $\frac{Pview(M,\alpha,\beta,\gamma)}{Pface(M,\alpha,\beta,\gamma)}$ can be used as a convexity measure for the 3D mesh M. But this ratio depends strongly on the choice of the coordinate system and, in some cases, it can be equal to 1 for concave meshes (see Figure 4(b)), which is not acceptable for a convexity measure. We address the problem by calculating $\min_{\alpha,\beta,\gamma\in[0,2\pi]} \frac{Pview(M,\alpha,\beta,\gamma)}{Pface(M,\alpha,\beta,\gamma)}$ instead of $\frac{Pview(M,\alpha,\beta,\gamma)}{Pface(M,\alpha,\beta,\gamma)}$ and define the new convexity measure of 3D meshes as

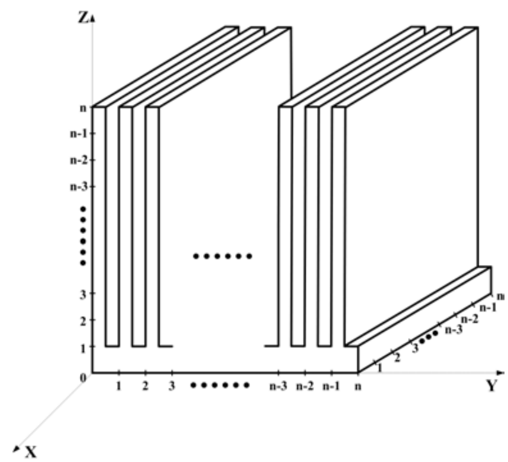

Figure 5. 3D polygon mesh M_n whose convexity measure $C(M_n)$ is arbitrarily close to 0, when n tends to infinity.

Definition 3. For a given 3D closed mesh M its convexity measure $C(M)$ is defined as

$$C(M) = \min_{\alpha,\beta,\gamma\in[0,2\pi]} \frac{Pview(M,\alpha,\beta,\gamma)}{Pface(M,\alpha,\beta,\gamma)}. \tag{7}$$

The following theorem summarizes properties of the proposed convexity measure:

Theorem 2. For any 3D mesh M, we have:

1. $C(M)$ is well defined and $C(M) \in (0,1]$;
2. $C(M) = 1$ if and only if M is convex;
3. $\inf_{M\in\Pi}(C(M)) = 0$, where Π denotes the set of all meshes;
4. $C(M)$ is invariant under similarity transformations.

Proof. Items 1, 2, 4 can be directly derived from Theorem 1 and Definition 3. In order to prove Item 3, we introduce a 3D mesh M_n (see Figure 5). Since the length of diagonal of the bounding box of M_n is $\sqrt{3}n$, which is the maximum length of line segments between any two points on M_n, we have

$$Pview(M,\alpha,\beta,\gamma) < 6 \cdot (\sqrt{3}n \cdot \sqrt{3}n) = 18n^2, \tag{8}$$

for any α,β,$\gamma \in [0, 2\pi]$. On the other hand

$$\begin{aligned} & Pface(M, \alpha, \beta, \gamma) \\ \geq \;& 6n^2 - 2 \cdot n \cdot \frac{1}{2} \cdot (n-1) + 2 \cdot (n-1) \cdot (n-1) \cdot n \\ = \;& 2n^3 + n^2 + 3n, \end{aligned} \tag{9}$$

and

$$\lim_{n \to \infty} \frac{18n^2}{2n^3 + n^2 + 3n} = 0, \tag{10}$$

which means, for any $\varepsilon > 0$, there exists a n such that

$$\begin{aligned} 0 \;&<\; C(M_n) = \min_{\alpha,\beta,\gamma \in [0,2\pi]} \frac{Pview(M_n, \alpha, \beta, \gamma)}{Pface(M_n, \alpha, \beta, \gamma)} \\ &<\; \frac{18n^2}{2n^3 + n^2 + 3n} < \varepsilon, \end{aligned} \tag{11}$$

or equivalently, for some M_n, their convexity $C(M_n)$ can be arbitrary close to 0. That completes the proof.

□

4. Computation of Convexity

In this section, we describe how to calculate the proposed convexity measure $C(M)$ for 3D meshes. We first present the computations of $Pface(M, \alpha, \beta, \gamma)$ and $Pview(M, \alpha, \beta, \gamma)$, and then we solve the nonlinear minimization problem to obtain an approximate value of the convexity measure. Note that, before the calculation of convexity, all models should be normalized with respect to the coordinate frame so that their mass centers coincide with the origin and they are bounded by the unit sphere.

4.1. Computation of $Pface(M, \alpha, \beta, \gamma)$

Assume that the 3D mesh M consists of N triangles $\{T_1, T_2, \ldots, T_N\}$. The coordinates of these triangles' vertices are denoted by (x_{i0}, y_{i0}, z_{i0}), (x_{i1}, y_{i1}, z_{i1}), (x_{i2}, y_{i2}, z_{i2}), $i = 1, \ldots, N$. After successively rotating the coordinate system around its x, y, z axes with angles α, β, γ, we obtain their new coordinates, which are denoted as $(x'_{i0}, y'_{i0}, z'_{i0})$, $(x'_{i1}, y'_{i1}, z'_{i1})$, $(x'_{i2}, y'_{i2}, z'_{i2})$, $i = 1, \ldots, N$, by using the following formulae

$$(x'_{ij}, y'_{ij}, z'_{ij})^T = R_z(\gamma) \cdot R_y(\beta) \cdot R_x(\alpha) \cdot (x_{ij}, y_{ij}, z_{ij})^T \qquad i = 1, \ldots, N; j = 0, 1, 2. \tag{12}$$

where $R_x(\alpha)$, $R_y(\beta)$, and $R_z(\gamma)$ stand for the matrixes which result in the rotations of the coordinate frame around its x, y, and z axes, respectively. Then, the sum of the three projected areas is computed by

$$Pface(M, \alpha, \beta, \gamma) = \sum_{i=1}^{N} \left(S'_{ix} + S'_{iy} + S'_{iz} \right), \tag{13}$$

where S'_{ix}, S'_{iy}, and S'_{iz} are the projected areas of the triangle T_i on the planes YOZ, ZOX, and XOY, respectively (see Figure 3).

Figure 6. A 2D projection of a 3D mesh. (a) is the exact shape of the projection while (b) is the silhouette view. Based on the number of black pixels in (c), area of the projected shape can be estimated.

4.2. Computation of $Pview(M, \alpha, \beta, \gamma)$

As mentioned in Section 3, $Pview(M, \alpha, \beta, \gamma)$ denotes the sum of areas of the valid regions in six views projected on faces of the bounding box whose edges are parallel to the coordinate axes. Theoretically, it is possible to calculate the exact area of the valid region shown in a 2D projection of a 3D polygon mesh. However, as shown in Figure 6(a), the boundary of a projected 2D polygon could be very complicated for some 3D meshes due to large amounts of overlapping and intersections. As a matter of fact, the complexity of the exact area calculation for this kind of 2D shapes is often unacceptable in practice. To solve the problem, we apply an image-based method to efficiently calculate the approximate value of $Pview(M, \alpha, \beta, \gamma)$. First, three silhouette views are captured in the directions of the coordinate axes (see Figure 6(b) for an example whose valid region is comprised of a set of black pixels). Then, we calculate the number of black pixels in three views (see Figure 6(c)), which are denoted as Np_x, Np_y, and Np_z, respectively. Note that the exact value of area of the projected image for each view is 4, since after normalization the mesh M is bounded by the unit sphere. Finally, let the total number of pixels in the view be denoted as Np, we have

$$\begin{aligned} & Pview(M, \alpha, \beta, \gamma) \\ = \;& 2 \cdot \left(4 \cdot \frac{Np_x}{Np} + 4 \cdot \frac{Np_y}{Np} + 4 \cdot \frac{Np_z}{Np} \right). \end{aligned} \tag{14}$$

Here, OpenGL is utilized to capture depth-buffer views from 3D objects and the resolution of images is experimentally chosen as 400×400, which implies $Np = 160000$.

4.3. Computation of $C(M)$

Owing to the complexity of $Pview(M, \alpha, \beta, \gamma)$ and $Pface(M, \alpha, \beta, \gamma)$, we find that it is very difficult and computationally expensive to compute the exact value of our convexity measure $C(M)$ for 3D meshes. On the other hand, according to the definition of $C(M)$, we observe that the computation of convexity is basically a nonlinear optimization problem which has been well studied and can be efficiently resolved by intelligent computing approaches.

In this paper, we choose the Genetic Algorithm (GA), which is an optimization technique based on natural evolution [6], to calculate the new convexity measure in the following two steps.

1. ***Initialization:*** Define and create a group with N_g individuals. Each individual contains a value of fitness $\frac{Pface(M,\alpha,\beta,\gamma)}{Pview(M,\alpha,\beta,\gamma)}$ and three chromosomes α,β, and γ, which are represented by binary codes.

2. ***Implementation:*** Iterate the genetic algorithm procedure, which consists of encoding, evaluation, crossover, mutation and decoding, for N_{gen} generations. The greatest value of fitness of all individuals in the group is obtained to calculate the approximate value of $C(M)$.

Coefficients of the Genetic Algorithm adopted here are selected as follows: the number of individuals $N_g = 50$; the number of evolution generations $N_{gen} = 200$; the length of each chromosome's binary codes $L_c = 20$; the probability of crossover $p_c = 0.800$ and mutation $p_m = 0.005$.

5. Convexity Distribution

According to the definition and theorems mentioned in Section 3, we know that the ratio

$$R(M,\alpha,\beta,\gamma) = \frac{Pview(M,\alpha,\beta,\gamma)}{Pface(M,\alpha,\beta,\gamma)} \tag{15}$$

relates closely to the convexity of a 3D mesh M. Since $R(M,\alpha,\beta,\gamma)$ changes when the rotation angles α,β,γ vary, a set of such ratios can be obtained by randomly (or uniformly) rotating the mesh around its center. We then construct a new shape descriptor CD (i.e., Convexity Distribution) based on the distribution of the above-mentioned ratios, which employs a histogram instead of a single value to better describe the convexity-related properties of 3D shapes compared to other existing convexity measurements. In this paper, rotation angles are chosen as random floating numbers between 0 to 2π, the number of rotations we make for a mesh is selected as $N_{rot} = 10000$, and the shape descriptor is built by quantizing these N_{rot} ratios $R(M,\alpha,\beta,\gamma)$ whose values range from 0 to 1 into a histogram with $N_{his} = 1024$ bins.

6. Results

To demonstrate the effectiveness of our convexity measurement, it is first applied to several specifically-designed 3D models which are obtained from a cube by cutting different numbers of thin cuboids. Figure 7 shows these models in order of their convexity values. As we can see, the more gaps an object has the smaller its convexity will be,

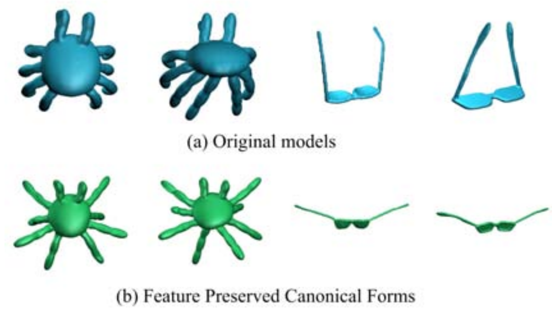

Figure 9. Non-rigid models (a) and their feature-preserved 3D canonical forms (b).

Table 1. Retrieval performance of our methods (CD and $C(M)$) and other convexity measures evaluated on the McGill database.

	NN	1-Tier	2-Tier	DCG
CD	57.3%	41.3%	67.1%	72.9%
$C(M)$	25.9%	26.3%	45.9%	60.4%
$C_1(M)$	27.8%	29.6%	51.9%	62.4%
$C_2(M)$	37.3%	26.0%	43.7%	59.8%

which coincides with our intuitive notion. Moreover, we also compute convexity values for other kinds of 3D meshes. Several examples are displayed in Figure 8, from which we observe that the proposed convexity measure is sensitive to the change of area and it generally corresponds well with human perception for the convexity of 3D objects.

Next, we apply our convexity measure and shape descriptor CD in the retrieval of non-rigid 3D shapes. Experiments are carried out on the widely-used McGill Articulated 3D Shape Benchmark [25], which consists of 10 categories containing 255 watertight meshes, and retrieval performance is evaluated by the Precision-recall plot as well as four quantitative measures (NN, 1-Tier, 2-Tier, DCG) [24]. Table 1 shows results for methods that utilize our approaches (i.e., CD and $C(M)$) and other two convexity measures (i.e., $C_1(M)$ and $C_2(M)$) to represent a 3D object and employ the L_1 norm to calculate the dissimilarity between two signatures. Note that all these convexity-related shape descriptors are computed on the canonical forms of the 3D meshes. As we can see from Figure 9, models in the same class may appear in quite different poses but can still have very similar canonical forms. Thereby, after the calculation of canonical forms, all feature extraction methods, even those specifically designed for rigid 3D shapes, can be employed to extract isometry-invariant shape descriptors from non-rigid objects. Here, we use a method recently presented in [10] to construct feature-preserved canonical forms for 3D meshes. As we can see from Table 1, representing a 3D object by a convexity measure that contains only a single value results in poor discrimination. While, because our shape descriptor CD provides more information to de-

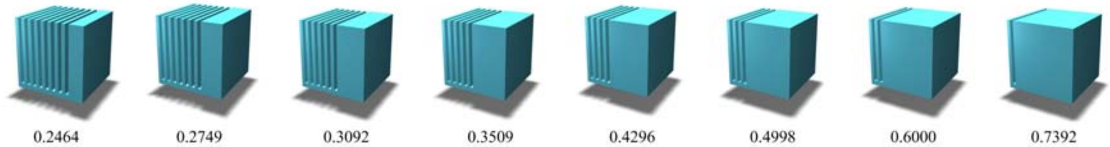

Figure 7. 3D meshes derived from a cube by cutting thin cuboids. Underneath are their convexity values obtained using our method.

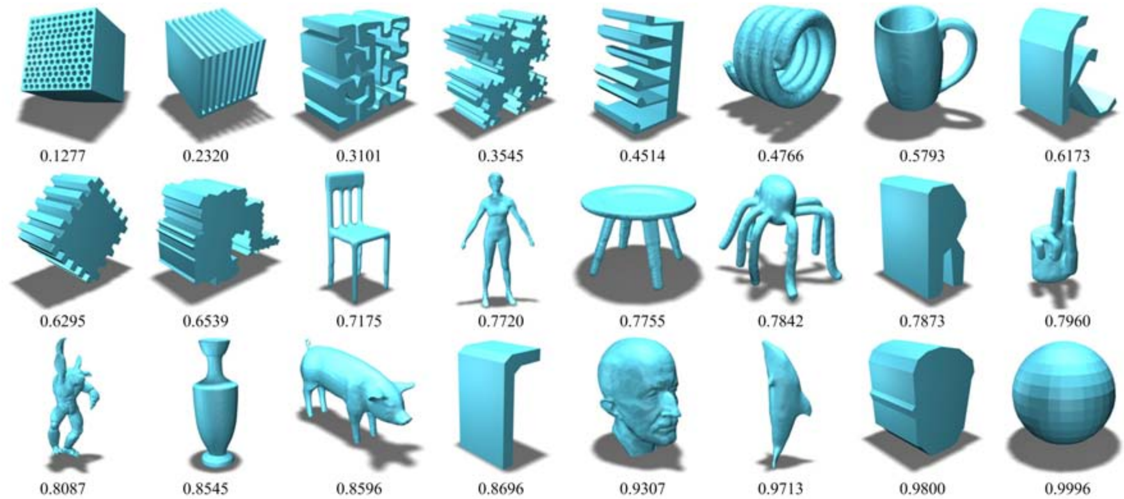

Figure 8. 3D shapes ranked by our convexity measure. Underneath are their corresponding convexity values.

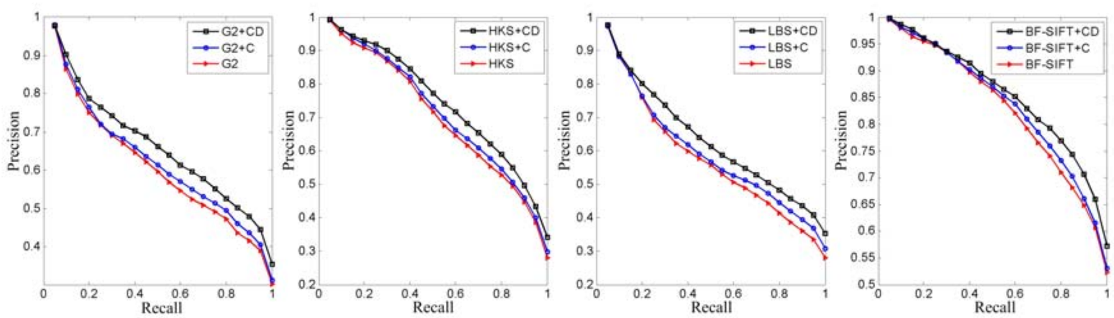

Figure 10. Precision-recall curves computed for 12 descriptors on the McGill benchmark. The precision-recall curves of a descriptor and its composite descriptors with the convexity measure (+C) and convexity distribution (+CD) are shown together in each subfigure.

scribe 3D shapes, it obtains much better performance compared to other convexity measures. Finally, we follow the method presented in [12] to generate 8 composite shape descriptors via the linear combination of our convexity-related shape descriptors (i.e., CD and $C(M)$) with the following isometry-invariant signatures: the shape distribution of Geodesic distance (G2) [13], Heat Kernel Signatures (HKS) [28], Laplace-Beltrami Spectrum (LBS) [20], and Bag-of-feature SIFT (BF-SIFT) [15]. Compared to the performance of original signatures, reasonable improvements in terms of retrieval accuracy have been achieved (see Figure 10), especially after combining with the new shape descriptor CD. This is mainly due to the fact that our convexity measure and our shape descriptor CD provide new and effective information, which is complementary with other existing signatures, to represent 3D shapes.

7. Conclusion

In this paper, a new convexity measure is developed for 3D meshes. The proposed convexity measure is defined based on the area of faces on the surface. Thereby, compared to the most commonly-utilized method (i.e., the ratio of the volume of a 3D object to the volume of its convex hull), it is more sensitive to deep indentations into objects, especially when the volume of these indentations are negligible. This is validated by our computed results which also demonstrate that the new convexity measure corresponds well with human intuition. The paper also proposes a convexity-related 3D shape descriptor based on the distribution of ratios $R(M, \alpha, \beta, \gamma)$ (Equation 15), which are computed by randomly rotating the mesh around its center, to better describe the object's convexity-related properties compared to existing methods. Finally, experiments were carried out on a widely-used benchmark to show the effectiveness of our convexity measure and the new shape descriptor in the application of non-rigid 3D shape retrieval.

Acknowledgements

This work was supported by National Natural Science Foundation of China under Grant 61073084, Beijing Natural Science Foundation of China under Grant 4122035, National Hi-Tech Research and Development Program (863 Program) of China under Grant 2012AA012503, National Key Technology Research and Development Program of China under Grants 2012BAH07B01 and 2012BAH18B03, and China Postdoctoral Science Foundation.

References

[1] L. Boxer. Computing deviations from convexity in polygons. *Pattern Recognition Letters*, 14(3):163–167, 1993. 2

[2] E. Bribiesca. An easy measure of compactness for 2d and 3d shapes. *Pattern Recognition*, 41(2):543–554, 2008. 2

[3] D.-Y. Chen, X.-P. Tian, Y.-T. Shen, and M. Ouhyoung. On visual similarity based 3D model retrieval. In *Proc. Eurographics 2003*, pages 223–232, 2003. 3

[4] A. Elad and R. Kimmel. On bending invariant signatures for surface. *IEEE PAMI*, 25(10):1285–1295, 2003. 3

[5] E. Fink and D. Wood. Fundamentals of restricted-orientation convexity. *Information Sciences*, 92(1):175–196, 1996. 2

[6] J. H. Holland. *Adaptation in Natural and Artificial Systems: An Introductory Analysis with Applications to Biology, Control and Artificial Intelligence*. MIT Press, 1992. 6

[7] A. E. Johnson and M. Hebert. Using spin images for efficient object recognition in cluttered 3d scenes. *IEEE PAMI*, 21(5):433–449, 1999. 3

[8] M. Kazhdan, T. Funkhouser, and S. Rusinkiewicz. Rotation invariant spherical harmonic representation of 3D shape descriptors. In *Proc. SGP'03*, pages 156–164, 2003. 2, 3

[9] J. Leou and W. Tsai. Automatic rotational symmetry determination for shape analysis. *Pattern Recognition*, 20(6):571–582, 1987. 1

[10] Z. Lian and A. Godil. A feature-preserved canonical form for non-rigid 3d meshes. In *Proc. 3DIMPVT 2011*, pages 116–123, 2011. 6

[11] Z. Lian, A. Godil, X. Sun, and H. Zhang. Non-rigid 3D shape retrieval using multidimensional scaling and bag-of-features. In *Proc. ICIP 2010*, pages 3181–3184, 2010. 3

[12] Z. Lian, P. L. Rosin, and X. Sun. Rectilinearity of 3D meshes. *IJCV*, 89(2-3):130–151, 2010. 3, 7

[13] M. Mahmoudi and G. Sapiro. Three-dimensional point cloud recognition via distributions of geometric distances. *Graphical Models*, 71(1):22–31, 2009. 3, 7

[14] F. Memoli and G. Sapiro. A theoretical and computational framework for isometry invariant recognition of point cloud data. *Foundations of Computational Mathematics*, 5(3):313–347, 2005. 3

[15] R. Ohbuchi, K. Osada, T. Furuya, and T. Banno. Salient local visual features for shape-based 3D model retrieval. In *Proc. SMI'08*, pages 93–102, 2008. 7

[16] R. Osada, T. Funkhouser, B. Chazelle, and D. Dobkin. Shape distributions. *ACM TOG*, 21(4):807–832, 2002. 3

[17] M. Petitjean. Chirality and symmetry measures: A transdisciplinary review. *Entropy*, 5:271–312, 2003. 1

[18] D. Proffitt. The measurement of circularity and ellipticity on a digital grid. *Pattern Recognition*, 15(5):383–387, 1982. 1

[19] E. Rahtu, M. Salo, and J. Heikkila. A new convexity measure based on a probabilistic interpretation of images. *IEEE PAMI*, 28(9):1501–1512, 2006. 1, 2

[20] M. Reuter, F. E. Wolter, and N. Peinecke. Laplace-spectra as fingerprints for shape matching. In *Proc. SPM'05*, pages 101–106, 2005. 7

[21] P. L. Rosin. Measuring rectangularity. *Machine Vision and Applications*, 11(4):191–196, 1999. 1

[22] P. L. Rosin. Measuring shape: ellipticity, rectangularity, and triangularity. *Machine Vision and Applications*, 14(3):172–184, 2003. 1

[23] P. L. Rosin and C. L. Mumford. A symmetric convexity measure. *Computer Vision and Image Understanding*, 103(2):101–111, 2006. 2

[24] P. Shilane, P. Min, M. Kazhdan, and T. Funkhouser. The princeton shape benchmark. In *Proc. SMI'04*, pages 167–178, 2004. 6

[25] K. Siddiqi, J. Zhang, D. Macrini, A. Shokoufandeh, S. Bouix, and S. Dickinson. Retrieving articulated 3d models using medial surfaces. *Machine Vision and Applications*, 19(4):261–275, 2008. 6

[26] M. Sonka, V. Hlavac, and R. Boyle. *Image Processing, Analysis, and Machine Vision*. Chapman and Hall, 1993. 2

[27] H. I. Stern. Polygonal entropy: A convexity measure. *Pattern Recognition Letters*, 10(4):229–235, 1989. 2

[28] J. Sun, M. Ovsjanikov, and L. Guibas. A concise and provably informative multi-scale signature based on heat diffusion. In *Proc. SGP'09*, pages 1383–1392, 2009. 7

[29] G. Tam and R. Lau. Deformable model retrieval based on topological and geometric signatures. *IEEE TVCG*, 13(3):470–482, 2007. 3

[30] J. W. Tangelder and R. C. Veltkamp. A survey of content based 3D shape retrieval methods. *Multimedia Tools and Applications*, 39(3):441–471, 2008. 3

[31] X. Wang, Y. Liu, and H. Zha. Intrinsic spin images: A subspace decomposition approach to understanding 3d deformable shapes. In *Proc. 3DPVT*, pages 17–20, 2010. 3

[32] J. Žunić, K. Hirota, and P. L. Rosin. A Hu moment invariant as a shape circularity measure. *Pattern Recognition*, 43(1):47–57, 2010. 1

[33] J. Žunić and P. L. Rosin. Rectilinearity measurements for polygons. *IEEE PAMI*, 25(9):1193–1200, 2003. 1

[34] J. Žunić and P. L. Rosin. A new convexity measure for polygons. *IEEE PAMI*, 26(7):923–934, 2004. 1, 2, 3